Hindawi
International Journal of Antennas and Propagation
Volume 2022, Article ID 8901752, 10 pages
https://doi.org/10.1155/2022/8901752

Research Article

Maximizing the Rate of IRS-Assisted Downlink NOMA Systems

Xinying Li, Haixia Wei, Haiyan Huang, Cuiran Li, and Lijun Zhang

School of Electronic and Information Engineering, Lanzhou Jiaotong University, Lanzhou 730070, China

Correspondence should be addressed to Xinying Li; 1824723674@qq.com

Received 26 January 2022; Revised 22 April 2022; Accepted 25 April 2022; Published 17 May 2022

Academic Editor: Stefano Selleri

Nonorthogonal multiple access (NOMA) techniques and intelligent reflecting surface (IRS) are being explored as potential essential technologies for future wireless communications. Accordingly, this paper provides a network framework for IRS-aided downlink NOMA transmission, in which IRS is employed to improve the NOMA system's transmission performance, and optimization problems are raised to maximize the achievable rate. Given the fractional structure of multivariate coupling as presented in this study, the fractional problem first converts to a linear form; then, the semidefinite relaxation (SDR) algorithm is proposed to address nonconvex issues for a single-user scenario. As for a multiuser scenario, the alternating optimization (AO) algorithm is raised based on transmit beamforming and reflection phase shift matrix to settle relevant issues and mitigate computational complexity. The simulation results suggest that the algorithm described in this paper can significantly increase the signal's achievable rate compared to the nondeployed IRS and IRS random phase-shifting schemes.

1. Introduction

In recent years, upgrading mobile communication systems have raised a higher demand for multiple access techniques [1]. Traditional cellular mobile communication systems mostly employ orthogonal multiple access (OMA) methods, which readily segregate the information conveyed by multiple user signals with little complexity. Nonetheless, the user amount supported by OMA is limited by the number of orthogonal resources available. Meanwhile, the orthogonality of the time-frequency code resources adopted in the system is frequently lost due to various impacts, such as time delay, frequency deviation, and Doppler Effect [2]. The nonorthogonal multiple access technique of new radio (NR) has been publicly discussed since the 3GPP RAN1#84bis meeting in April 2016, followed by various proposed schemes regarding NOMA techniques in recent years. Li A. Lan Y et al., for instance, offered a downlink NOMA scheme using successive interference cancellation (SIC) receivers and demonstrated in the paper that the scheme should enhance the capacity and cell edge user throughput, whose performance improvement is irrelevant to the availability of the frequency selective channel quality indicator (CQI) on the base station side [3, 4]. In order to improve large-scale connectivity, Mounchili and Hamouda investigated the minimal pairing distance to distinguish between far and near users; an analytical expression of the distance threshold on pairing was presented in the case of fixed power allocation [5]. During this time, researchers also proposed a slew of other advanced communication technologies, such as Terahertz (THz) communication, large-scale Multiple Input Multiple Output (MIMO) [6, 7], Ultradense Network (UDN) [8, 9], and so on, all of which greatly support the spectral efficiency of wireless communication systems. However, widespread adoption of these technologies necessitates high hardware costs and significant energy consumption, which has driven the wireless communication domain to pursue better data transmission speeds and spectral efficiency while imposing higher demands on the system's energy efficiency [10]. Besides, the intelligent reflecting surface is perceived as a possible technical solution for further lowering wireless network costs with increasing energy efficiency [11–14].

As communication technology is evolving, researchers have begun to integrate IRS with NOMA techniques to upgrade the performance of the communication system and are committed to relevant studies regarding the optimization of IRS-aided NOMA communications systems. Long et al.

provided an overview of IRS, including the signal model, hardware architecture, and challenges of IRS application and deployment in 6G networks [15]. Wu et al. explain reflection and channel models, hardware architecture, and practical limitations of IRS-assisted wireless communication, as well as a variety of attractive applications in wireless networks. In addition, they highlight important directions worthy of further research in future work [13]. de Sena et al. summarized the main roles and key challenges of IRS in MIMO-NOMA systems and gave a comprehensive discussion of the main performance gains that can be achieved in IRS-assisted large-scale MIMO-NOMA networks and outlined the future use scenarios of IRS-NOMA systems. The main challenges and future research directions are also revealed [16]. Fang et al. studied an IRS-assisted downlink MISO-NOMA system to optimize system energy efficiency by jointly optimizing the transmitting beam shaping of BS and the reflected beam shaping of IRS [17]. Zhu et al. developed an IRS-aided MISO-NOMA system that effectively adjusts the wireless channel; it further minimizes the transmission power by optimizing the beamforming vector and the IRS phase shift matrix. Moreover, an enhanced quasi-degradation is proposed using IRS, ensuring that NOMA reaches the capacity region with a higher probability [18]. Cheng et al. studied a downlink NOMA system that expands base station coverage by increasing the number of IRS deployments and derives the diversity order pursuant to the asymptotic approximation in the range of high signal-to-noise ratio [19]. In response to dual-cell IRS-aided NOMA system with joint detection, Wang et al. put forward an uplink power minimization issue to realize joint optimization of the system's power allocation and phase shift [20]. Ding and Vincent Poor highlighted the IRS-NOMA transmission scheme for a multiuser NOMA downlink scenario, assuming no direct link exists between the base station and cell-edge users. This scheme permits to serve more users in each direction of orthogonal space than the space division multiple access schemes. Also, the impact of hardware damage on IRS-NOMA is incorporated in their studies [21]. They also investigated the effect of two phase shift designs, coherent phase shift, and random discrete phase shift, on the performance of IRS-assisted NOMA [22]. In addition, Mu et al. studied ideal and nonideal RIS-assisted multiple input and multiple output scenarios and further proposed a new NOMA decoding order [23].

IRS can be divided into active IRS and passive IRS. In the scenario where the direct link between the transmitter and receiver is strong, since the active IRS is equipped with an additional integrated active reflection-type amplifier, the reflective element has the function of amplifying the signal, which will strengthen the reflective link. However, with active components, the IRS needs to consume extra power to amplify the signal, and the thermal noise introduced by the active IRS cannot be ignored like the passive IRS. Passive IRS consume virtually zero direct-current power and can be used to send pilot signals and process baseband signals, whereas active IRS do not have this capability and can only reflect and amplify the signal to strengthen the reflected link [24]. So, this paper uses passive IRS auxiliary signal transmission.

An antenna array has been formed by transmitting antennas due to the adoption of NOMA technology; in this case, regarding the devices used to achieve beamforming, such as equipping antennas with digital-to-analog converters, the cost of the system will increase. The intelligent reflecting surface (IRS) comprises numerous low-cost passive reflecting units, and it actively modifies the wireless communications environment to enhance network performance. In summary, associating IRS with NOMA techniques has become a principal research focus since both are expected to play active roles as potential essential technologies in future wireless communications. Yet, the rate optimization issue of the IRS-aided NOMA system has received little attention in academic research. In the case of bounded channel's uncertainty, research on the algorithm of IRS-aided NOMA system's rate maximization comes with theoretical significance. Therefore, this paper makes contributions to propose a network framework for IRS-aided NOMA downlink transmission. Multiple users can share the same resource block simultaneously; drawing upon IRS, it is viable to enhance the transmission performance of the NOMA system by adjusting the wireless communication channel. The problem of maximizing the achievable signal rate is proposed; meanwhile, the relationship between the power distribution coefficient and the reflection phase shift matrix is derived while meeting the limitations of maximum transmission power and reflection unit phase shift. Since the problem is involved in a fractional structure of multivariate coupling, the solving process is quite challenging. This study first reduces the complex fractional problem to a linear problem and proposes a semidefinite relaxation (SDR) technique based on maximum ratio transmission (MRT) to solve nonconvex problems for single-user scenarios. Then, in respect of multiuser scenarios, a minimum mean squared error (MMSE) estimator is applied to cope with multiuser interference between multiantenna access points. Besides, the alternating optimization algorithm is put forward based on transmit beamforming and the reflection phase shift matrix to reduce computational complexity. Furthermore, the IRS can only reflect the signal, while signal transmission suffers from significant path loss due to the sophisticated communications environment. On the other hand, given the simple installation of IRS, the free-space model is exploited to deploy the IRS in a position with a direct path to the base station. It also keeps a relatively close distance to the region to be enhanced, adjusts the phase of each reflecting unit on the reflective display panel, and reduces the path loss via the convergence function. The simulation findings show that the SDR and AO schemes presented in the paper can dramatically enhance the achievable rate of the IRS-aided NOMA downlink system, along with the rate value growing as the number of IRS reflection units increases.

2. System Model

As presented in Figure 1, the proposed IRS aims to aid the NOMA system in completing downlink transmission, in which a base station (BS) with N number of antennas, an IRS with L number of passive reflection units, and M number of

users (User, UE) are deployed. The channel response parameters of the link from the base station to the intelligent reflecting surface, from the intelligent reflecting surface to the user i, and from the base station to the user i are represented by $H \in C^{L\times N}$, $g_{r,i}^{H} \in C^{1\times L}$ and $h_{r,i}^{H} \in C^{1\times N}$, respectively, where $i \in \{1, 2, ..., M\}$.

The user set is described as $\overline{M} = \{1, 2, ..., M\}$ while the channel set is $\overline{N} = \{1, 2, ..., N\}$. The total system bandwidth B is evenly allocated to a set of channels, and the bandwidth of each channel is presented as $W = (B/N)$. According to the power multiplexing techniques of NOMA, multiple users can be allocated on a subchannel to achieve frequency sharing. Supposing each user is assigned to one channel, t_n denotes the number of users distributed on the n-th channel while T_n signifies the maximum number of users possible to be allocated on each channel. When $T_n = 1$, the IRS-NOMA system is transformed into the IRS-OMA system. The IRS reflection coefficient matrix is indicated as Θ, $\Theta \in C^{L\times L}$ while $\Theta = di\ ag\{A_1 e^{j\theta_1}, A_2 e^{j\theta_2}, ..., A_L e^{j\theta_L}\}$. In the formula, $A_l e^{j\theta_l}$ represents the reflection coefficient of the l-th reflection unit, θ_l reflects the phase coefficient of the l-th reflection unit while $\theta_l \in [0, 2\pi]$, and A_l represents the reflection coefficient of the l-th reflection unit while $A_l \in [0, 1]$. The following scenarios can be considered for IRS phase optimization: modulating the phase, modulating the amplitude, or modulating both simultaneously. A simple circuit features the choice of merely modulating the amplitude while its performance seems poor. Yet, modulating both phase and amplitude contributes to improved performance, while the hardware design can be highly complicated. Therefore, the available research can only modulate the stage, thereby achieving an ideal balance between performance and complexity [25]. It is assumed that each reflection unit on the IRS performs maximum reflection; that is, the amplitude coefficient of each reflection unit conforms to $A_1 = A_2 = ... = A_L = 1$.

For passive IRS, the reflection unit has no sensing element installed, so the IRS cannot receive pilot signals directly from BS and UE. The system adopts a full duplex (FD) mode, as shown in Figure 2, each transmission frame (T_L) is divided into two transmission stages. In the first transmission phase ($T_{L1} \ll T_L$), UE sends pilot signals to BS through the uplink channel, and IRS changes the reflection coefficient in real time according to the preset reflection mode to reflect the pilot signals sent by UE to BS. BS receives a dual-link pilot signal that contains both a direct link and a reflected link. Based on these signals, BS estimates the direct link UE-BS and the reflected link UE-IRS-BS. Then, BS uses the estimated channel state information (CSI) to transmit the passive beam configuration parameters to IRS through the feedback link. The transmitted beam configuration of BS and the reflection phase shift matrix of IRS are jointly designed to realize data transmission. Assuming that all channels are quasi-static flat fading channels, due to the reciprocity of channels, CSI obtained by uplink pilot training can also be used for downlink data transmission. In the second transmission phase ($T_{L2} \triangleq T_L - T_{L1}$), IRS sets the reflection phase shift matrix according to the passive beam

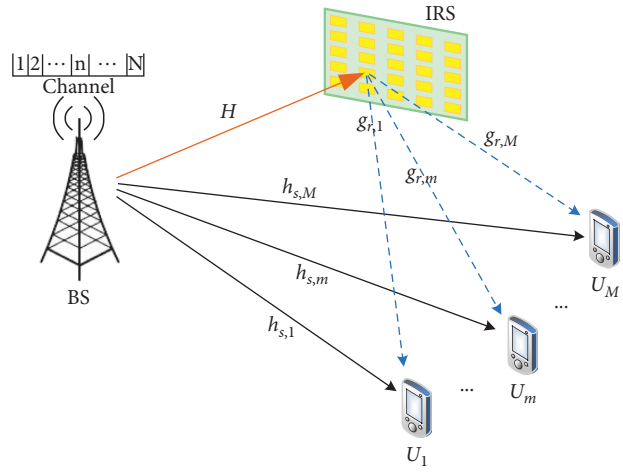

Figure 1: Block diagram of the system model.

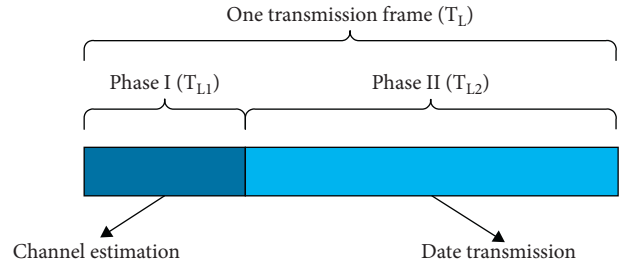

Figure 2: Transmission mode.

configuration parameters fed back by BS to assist in downlink data transmission between BS and UE.

The signal will have a large path loss in the process of multiple reflection transmission, assuming that the signal reflected by IRS two or more times is ignored. In addition, in order to facilitate the theoretical performance gain brought by IRS, it is assumed that BS knows all channel state information, which can be obtained by the method in reference [26].

The signal received by the user U_m is as follows:

$$y_m = \left(g_{r,m}^{H}\Theta H + h_{s,m}^{H}\right)\sum_{i=1}^{M} w_i s_i + e_m,\ \forall m \in \overline{M}, \tag{1}$$

where w_i represents the beamforming vector of the user i, s_i represents the signal transmitted by BS to U_i, and e_m denotes additive white Gaussian noise with a mean value of 0 and a variance of σ^2 [27].

As presented in Figure 3, NOMA adopts the serial interference cancellation technique at the receiving end [28]. Specifically, the user U_1 directly decodes the signal s_i after receiving the signals and treats the remaining signals as noise. When $m \geq 2$, the user detects the received signals individually; later, it restores the signal amplitude and detects the remaining signals after excluding the detected signals of other users from the received signal. This operation continues to repeat until the demanded signals are decoded.

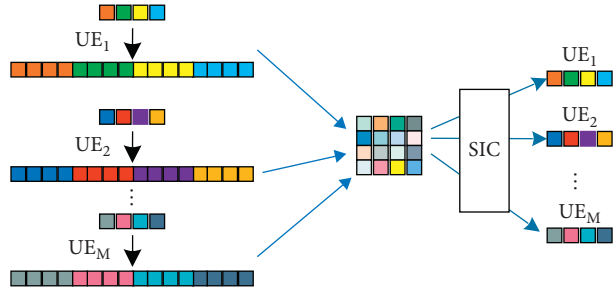

Figure 3: SIC schematic diagram.

The sequence of M number of users is $\|h_{s,1}\|_2 \le \|h_{s,2}\|_2 \le \ldots \|h_{s,M}\|_2$, where $\|h_{s,m}\|_2$ signifies the channel quality between user U_m and BS. Therefore, the signal of the user U_m before decoding the signal can be denoted as follows:

$$y_m' = \left(g_{r,m}^H \Theta H + h_{s,m}^H\right) \sum_{i=m}^{M} w_i s_i + e_m, \forall m \in \overline{M}. \tag{2}$$

The signal-to-noise ratio of the user U_m's decoded signal s_m is indicated as follows:

$$\mathrm{SINR}_m = \frac{\left|\left(g_{r,m}^H \Theta H + h_{s,m}^H\right) \cdot w_m\right|^2}{\sum_{i=m+1}^{M} \left|\left(g_{r,m}^H \Theta H + h_{s,m}^H\right) \cdot w_i\right|^2 + \sigma^2}, \quad \forall m \in \overline{M}. \tag{3}$$

According to Shannon's theorem [29], the achievable rate of the user U_m receiving signal s_m is presented as follows:

$$R_m = \log_2\left(1 + \mathrm{SINR}_m\right) = \log_2\left(1 + \frac{\left|\left(g_{r,m}^H \Theta H + h_{s,m}^H\right) \cdot w_m\right|^2}{\sum_{i=m+1}^{M} \left|\left(g_{r,m}^H \Theta H + h_{s,m}^H\right) \cdot w_i\right|^2 + \sigma^2}\right), \quad \forall m \in \overline{M}. \tag{4}$$

Therefore, the throughput of the system is expressed as follows:

$$R_{sys} = \sum_{m=1}^{M} \log_2\left(1 + \mathrm{SINR}_m\right) = \sum_{m=1}^{M} \log_2\left(1 + \frac{\left|\left(g_{r,m}^H \Theta H + h_{s,m}^H\right) \cdot w_m\right|^2}{\sum_{i=m+1}^{M} \left|\left(g_{r,m}^H \Theta H + h_{s,m}^H\right) \cdot w_i\right|^2 + \sigma^2}\right). \tag{5}$$

3. Scheme Design for Maximizing the Transmission Rate

When the transmit power meets the constraints, alternating optimization is conducted on the BS's active transmit beamforming and the IRS's passive reflection phase shift, allowing the NOMA system to reach the maximum rate during downlink transmission.

3.1. Problem Modeling. The optimization problem can be stated as follows:

$$\begin{aligned} \mathrm{P}_1: \max_{w,\Theta} & \log_2\left(1 + \frac{\left|\left(g_{r,m}^H \Theta H + h_{s,m}^H\right) \cdot w_m\right|^2}{\sum_{i=m+1}^{M} \left|\left(g_{r,m}^H \Theta H + h_{s,m}^H\right) \cdot w_i\right|^2 + \sigma^2}\right) \\ \text{s.t. } & 0 \le \theta_l \le 2\pi, l = 1, 2, \ldots, L, \\ & \sum_{m=1}^{M} \|w_m\|^2 \le P_{\max}, \end{aligned} \tag{6}$$

where $P_{\max}$ refers to the maximum transmit power offered by BS.

The solving process can be challenging since the objective function and constraints are nonconvex [30]. To simplify the calculation, the single-user scenario is initially considered, followed by a semidefinite relaxation technique to approximate the solution; afterward, extending this process to the multiuser scenario with an AO algorithm for problem solving.

3.2. Single-User System. We consider a single-user system, i.e., $M = 1$, in this case, the system is comparable to IRS-OMA. Besides, there is no mutual interference while only one user is in the system; hence, problem P_1 can be reduced to the following:

$$\begin{aligned} \mathrm{P}_2: \max_{w,\Theta} & \log_2\left(1 + \frac{\left|\left(g_r^H \Theta H + h_s^H\right) \cdot w\right|^2}{\sigma^2}\right) \\ \text{s.t. } & 0 \le \theta_l \le 2\pi, l = 1, 2, \ldots, L, \\ & \|w\|^2 \le P_{\max}. \end{aligned} \tag{7}$$

Regarding the analysis of the problem P_2, when the signal-to-noise ratio takes the maximum value, the system's achievable rate reaches the maximum accordingly; thus, the problem P_2 is equivalent to the following:

$$\begin{aligned} \mathrm{P}_3\text{:}\ & \max_{w,\Theta} \frac{\left|\left(g_r^H \Theta H + h_s^H\right)\cdot w\right|^2}{\sigma^2} \\ & \text{s.t. } 0 \le \theta_l \le 2\pi, l = 1, 2, ..., L, \\ & \|w\|^2 \le P_{\max}. \end{aligned} \tag{8}$$

As variable coupling exists in the objective function of P_3, the problem P_3 is regarded as nonconvex. The transmit beam at BS and the phase shift matrix at IRS are alternately optimized until convergence. In addition, w remains constant before solving Θ. The problem P_3 can be simplified to as follows:

$$\begin{aligned} \mathrm{P}_4\text{:}\ & \max_{\theta} \frac{\left|\left(g_r^H \Theta H + h_s^H\right)\cdot w\right|^2}{\sigma^2} \\ & \text{s.t. } 0 \le \theta_l \le 2\pi, l = 1, 2, ..., L. \end{aligned} \tag{9}$$

Let $\widetilde{v} = [v_1, v_2, ..., v_L]^H$, where $v_l = e^{j\theta_l}, \forall l$. Thus, the constraints in P_4 can be equivalent to the unit modulus constraint: $|v_l|^2 = 1, \forall l$. Using variables to replace: $g_r^H \cdot \Theta \cdot H = \widetilde{v} \cdot \Phi$, $\Phi = di\,ag(g_r^H) \cdot H \in C^{L\times N}$ and $\xi = (P/\sigma^2)$, then problem P_4 is equivalent to the following:

$$\begin{aligned} \mathrm{P}_5\text{:}\ & \max_{\widetilde{v}} \xi \cdot \widetilde{v}^H \cdot \Phi \cdot \Phi^H \cdot \widetilde{v} + \xi \cdot \widetilde{v}^H \cdot \Phi \cdot h_s^H + \xi \cdot h_s^H \cdot \Phi^H \cdot \widetilde{v} + \xi \cdot \left\|h_s^H\right\|^2 \\ & s.t. \left|v_l\right|^2 = 1, l = 1, 2, ..., L. \end{aligned} \tag{10}$$

Problem P_5 is a nonconvex quadratically constrained quadratic programming (QCQP) [31], which can be reformulated as homogeneous QCQP. Specifically, the auxiliary variable t is introduced, allowing the problem P_5 to be equivalently rewritten as follows:

$$\begin{aligned} \mathrm{P}_6\text{:}\ & \max_{\overline{v}} \overline{v}^H \cdot R \cdot \overline{v} + \xi \cdot \left\|h_s^H\right\|^2 \\ & \text{s.t. } \left|v_l\right|^2 = 1, l = 1, 2, ..., L. \end{aligned} \tag{11}$$

In the formula, $\widetilde{R} = \begin{bmatrix} \Phi \cdot \Phi^H & \Phi \cdot h_s^H \\ h_s^H & 0 \end{bmatrix}$, $\overline{v} = \begin{bmatrix} \widetilde{v} \\ t \end{bmatrix}$, $R = \xi \cdot \widetilde{R}$. The problem P_6 remains nonconvex here; the applied formula is $\overline{v} \cdot \widetilde{R} \cdot \overline{v}^H = tr(\widetilde{R} \cdot \overline{v} \cdot \overline{v}^H)$, let $V = \overline{v} \cdot \overline{v}^H$, and V needs to meet $V \ge 0$ while rank $(V) = 1$. Since the rank one constraint is non-convex, SDR is used to relax this constraint. Question P_6 is simplified to the following:

$$\begin{aligned} \mathrm{P}_7\text{:}\ & \max_{V} tr(R \cdot V) + \xi \cdot \left\|h_s^H\right\|^2 \\ & \text{s.t. } V_{l,l} = 1, l = 1, 2, ..., L, \\ & V \ge 0. \end{aligned} \tag{12}$$

Since problem P_7 is convex semidefinite programming (SDP), the optimal solution can be obtained through CVX [32].

The beamforming of the base station is ready to be optimized once the reflection coefficient matrix Θ of the IRS has been optimized. For any given θ, the optimal transmission beamforming is solved by maximum ratio transmission (MRT) [33], let $\widetilde{w} = \sqrt{P} \cdot (g_r^H \cdot \Theta \cdot H + h_s^H)^H / \|g_r^H \cdot \Theta \cdot H + h_s^H\|$, where P represents the base station's transmit power. Problem P_7 is equivalent to the following:

$$\begin{aligned} \mathrm{P}_8\text{:}\ & \max_{P} \delta \cdot P \\ & \text{s.t. } P \le P_{\max}. \end{aligned} \tag{13}$$

In the formula, $\delta = |g_r^H \cdot \Theta \cdot H + h_s^H|^2/\sigma^2$. At this point, we have transformed the optimization goal in passive beamforming into the standard positive semidefinite programming in (12), which can be optimized through CVX toolbox.

Typically, the relaxed problem P_8 may not necessarily obtain a rank one solution, i.e., rank $(V) \ne 1$. This means that the optimal target value of problem P_8 only describes the upper limit of P_7. Hence, an additional solution step is required to construct an effective suboptimal solution of problem P_8 from the objective function of problem P_8. Decompose V by randomization, let $V = QAQ^H$, where $Q = [e_1, e_2, \cdots, e_L]$ is a unitary matrix and $A = [\lambda_1, \lambda_2, \cdots, \lambda_L]$ is a diagonal matrix, both of size $L \times L$, and then obtain a suboptimal solution of problem P_6. Let $\overline{v} = QA^{1/2}x$, where $x \in C^{L\times 1}$ is a random vector generated by $CN(0, I_L)$, and $CN(0, I_L)$ is a circularly symmetric complex Gaussian(CSCG) distribution with a mean of 0 and a variance of I_L. Since the Gaussian random vector x is independent, the target value of problem P_6 is approximately the maximum reached by the best $\overline{v}$ of all x. Given enough random numbers, the SDR algorithm can ensure that $(\pi/4)$ is used to approximate the optimal target value of problem P_7. SDR is an approximate solution algorithm that eliminates the rank-one constraint. Compared with Lagrange algorithm, although the computational complexity is higher, but its solution accuracy is higher, so the SDR algorithm is often used in convex optimization solution.

3.3. Multiuser Scenario. Multiuser $(M > 1)$ scenario is considered on the basis of the single-user scenario. Unlike the maximum ratio transmission criterion adopted in the single-user condition without interference, the minimum mean square error (MMSE) [34] estimator is used to describe the transmit beamforming at BS in the multiantenna access point scenario. In addition, because the receiver in NOMA system uses SIC technology, the BS allocates

stronger transmitting power to users with poor channel quality. The receiver decoding is also demodulated preferentially. After demodulation is completed, the modulated signals are deleted from the superimposed signals, and so on until all users have completed signal demodulation. With the maximum signal-to-noise ratio of the signal, the achievable rate is maximized accordingly. Thus, when the BS's transmit beamforming is determined, the problem P_1 is simplified to the following:

$$P_9: \max_{\theta} \frac{\left|\left(g_{r,m}^H \cdot \Theta \cdot H + h_{s,m}^H\right) w_m\right|^2}{\sum_{i=m+1}^{M} \left|\left(g_{r,m}^H \cdot \Theta \cdot H + h_{s,m}^H\right) w_i\right|^2 + \sigma^2} \quad (14)$$

$$\text{s.t. } 0 \le \theta_l \le 2\pi, l = 1, 2, \ldots, L.$$

Let $\overrightarrow{v} = [v_1, v_2, \ldots, v_L]$, where $v_l = e^{j\theta_l}, \forall l$. The constraints in problem P_9 are equivalent to $|v_l|^2 = 1, \forall l$. The applied substitution variables are presented as $\phi_{m,j} = di\ ag(g_{r,m}^H) \cdot H \cdot w_j \in C^{L \times N}$, then $g_{r,m}^H \cdot \Theta \cdot H \cdot w_j = \overrightarrow{v}^H \cdot \phi_{m,j}$, $h_{s.m}^H \cdot w_j = \varepsilon_{m,j}$, and $\|(g_{r,m}^H \cdot \Theta \cdot H + h_{s,m}^H) \cdot w_m\|^2 = \|\overrightarrow{v} \cdot \phi_{m,m} + \varepsilon_{m,m}\|^2$, the problem P_9 hence is simplified to as follows:

$$P_{10}: \max_{\theta} \frac{\overrightarrow{v}^H \cdot \phi_{m,m} \cdot \phi_{m,m}^H \cdot \overrightarrow{v} + \overrightarrow{v}^H \cdot \phi_{m,m} \cdot \varepsilon_{m,m}^H + \varepsilon_{m,m} \cdot \phi_{m,m}^H \cdot \overrightarrow{v} + \left|\varepsilon_{m,m}^H\right|^2}{\sum_{i=m+1}^{M} \left(\overrightarrow{v}^H \cdot \phi_{m,i} \cdot \phi_{m,i}^H \cdot \overrightarrow{v} + \overrightarrow{v}^H \cdot \phi_{m,i} \cdot \varepsilon_{m,i}^H + \varepsilon_{m,i} \cdot \phi_{m,i}^H \cdot \overrightarrow{v} + \left|\varepsilon_{m,i}^H\right|^2\right) + \sigma^2} \quad (15)$$

$$\text{s.t. } |v_l|^2 = 1, l = 1, 2, \ldots, L.$$

Yet, problem P_{10} remains a nonconvex quadratically constrained quadratic programming problem; thus, the SDR technique will be used to approximate this problem. Specifically, the auxiliary variable t is introduced, let $\overline{v} = \begin{bmatrix} \overrightarrow{v} \\ t \end{bmatrix}$, $R_{m,j} = \begin{bmatrix} \phi_{m,j} \cdot \phi_{m,j}^H & \phi_{m,j} \cdot \varepsilon_{m,j}^H \\ \phi_{m,j}^H \cdot \varepsilon_{m,j} & 0 \end{bmatrix}$, and the problem P_{10} is rewritten as follows:

$$P_{11}: \max_{\overline{v}} \frac{\overline{v}^H \cdot R_{m,m} \cdot \overline{v} + \left|\varepsilon_{m,m}\right|^2}{\sum_{i=m+1}^{M} \left(\overline{v}^H \cdot R_{m,i} \cdot \overline{v} + \left|\varepsilon_{m,i}\right|^2\right) + \sigma^2} \quad (16)$$

$$\text{s.t. } |v_l|^2 = 1, l = 1, 2, \ldots, L.$$

The formula $\overline{v} \cdot R_{m,j} \cdot \overline{v}^H = tr(R_{m,j} \cdot \overline{v} \cdot \overline{v}^H)$ is applied with $V = \overline{v} \cdot \overline{v}^H$ defined, and V is required to meet $V \ge 0$ while rank $(V) = 1$; relaxing the constraints, and the problem P_{11} is further turned into the following:

$$P_{12}: \max_{V} \frac{tr\left(R_{m,m} \cdot V\right) + \left|\varepsilon_{m,m}\right|^2}{\sum_{i=m+1}^{M} \left(tr\left(R_{m,i} \cdot V\right) + \left|\varepsilon_{m,i}\right|^2\right) + \sigma^2} \quad (17)$$

$$\text{s.t. } V_{l,l} = 1, l = 1, 2, \ldots, L, V \ge 0.$$

It is noticed that the problem P_{12} is a common positive semidefinite programming problem whose optimal solution can be obtained through the existing CVX toolbox.

According to the above optimization of the achievable rate of the user's signal, the maximum throughput of the system can be expressed as follows:

$$P_{13}: \max_{V} \sum_{m=1}^{M} \frac{tr\left(R_{m,m} \cdot V\right) + \left|\varepsilon_{m,m}\right|^2}{\sum_{i=m+1}^{M} \left(tr\left(R_{m,i} \cdot V\right) + \left|\varepsilon_{m,i}\right|^2\right) + \sigma^2} \quad (18)$$

$$\text{s.t. } V_{l,l} = 1, l = 1, 2, \ldots, L, V \ge 0.$$

4. Simulation Result Analysis

In this section, the influence of the SDR algorithm and AO algorithm proposed in the article on the signal's achievable rate is verified. It is compared with the following two schemes: (1) IRS random phase-assisted NOMA downlink transmission system: the phase shift of channel H and $g_{R,m}$ is a random value in the range of $[0, 2\pi]$. Then, MRT is performed at the BS according to the combined channel to maximize the signal achievable rate; (2) Non-IRS-aided NOMA downlink transmission system: Set the model as IRS is absent, based on $w = P(h_s/\|h_s\|)$. Then, the BS optimizes transmit beamforming according to the CSI of the channel BS-UE to maximize the signal achievable rate.

4.1. Simulation Parameter Settings. The reference center antennas at BS and IRS are, respectively, set to (0,0) and (60m,60 m) in the two-dimensional coordinate system. The system's path loss model is expressed as follows:

$$L(d) = C_0 \left(\frac{d}{D_0}\right)^{-\alpha}, \quad (19)$$

where C_0 denotes the path loss at a distance $D_0 = 1$, d reflects the distance, and α signifies the path loss index. With the ignorance of their heights, the distances between BS and IRS,

IRS and UEs, and BS and UEs are represented by d_1, d_2, d_3 respectively. The amplitude attenuation coefficients of channels H, $g_{R,m}$, and $h_{s,m}$ are described as $\sqrt{L_1} = \sqrt{C_0 (d_1/D_0)^{-\alpha_1}}$, $\sqrt{L_2} = \sqrt{C_0 (d_2/D_0)^{-\alpha_2}}$, and $\sqrt{L_3} = \sqrt{C_0 (d_3/D_0)^{-\alpha_3}}$ respectively; where $C_0 = -30$ dB, the path loss index of the channel between BS and IRS is set as $\alpha_1 = 2$, i.e., the free space fading model. The path loss index of the channel between IRS and UEs is set as $\alpha_2 = 2.8$, and the path loss index of the channel directly connected between BS and UEs is set as $\alpha_3 = 3.5$.

Assuming that the channels involved in the simulation process all conform to the Rician fading channel model, the channel H between BS-IRS is as follows:

$$H = \sqrt{\frac{\beta_1}{1+\beta 1}} H^{LoS} + \sqrt{\frac{1}{\beta_1 + 1}} H^{NLoS}, \tag{20}$$

where β_1 denotes the fading coefficient, H^{LoS} signifies a certain visible path, and H^{NLoS} refers to the Rayleigh fading channel. When β_1 tends to infinity, the channel model is simplified into a LoS channel; by contrast, when β_1 tends to 0, the channel model is simplified into a Rayleigh channel. Then, multiply H by the square root of the distance-dependent path loss in (19). β_2 and β_3 are, respectively, applied to reflect the channel fading coefficients of the two links known as IRS-UEs and BS-UEs. $\beta_1 = \infty$ is set, which means the channel between BS-IRS is the LoS path; $\beta_2 = \beta_3 = 0$, so there is a Rayleigh scenario between IRS-UEs and BS-UEs. Other simulation parameters are shown in Table 1.

4.2. Simulation Analysis. Figure 4 displays the condition when ten users are randomly placed in a circle with the center $(d, 10)$ and a radius of 5m, it further reflects the signals' achievable rate required by the users at various d values. In addition, three outcomes are noticed in the figure. First and foremost, it can be discovered that the signal achievable rate of the NOMA downlink system with IRS aid is higher than the signal achievable rate of the NOMA downlink system without IRS support. The IRS function is to enhance desired signals while suppressing interference signals. Second, it is obvious that compared to the scheme with absent IRS, the two optimization algorithms adopted present a remarkable peak when $d = 60m$, showing that in the case of adopting these two optimization schemes, when the distance between the user and the IRS is the smallest, the achievable signal rate will be the highest; because at this time, the reflected signal received by the user is the strongest, and a peak will not appear in the scheme without IRS. Finally, it can be seen that the achievable signal rates of the IRS random phase system and the system without IRS aid are sufficiently proximate; this is due to the IRS with missing passive beamforming, which cannot accurately reflect the signal received by the BS to a specific user.

Figure 5 depicts the relationship between the achievable signal rate and the distance between the user and the IRS using the AO scheme. At the same time, different numbers of transmitting antennas are set in BS. Based on the simulation results, it is summarized that the signal's achievable rate

Table 1: Simulation parameters.

Parameter	Numerical
Number of UEs(M)	10
Number of antennas of the BS(N)	8
Number of elements at IRS(L)	100
Number of antennas per UE(U)	2
Noise power (σ^2)	−80 dBm
Distance between BS-IRS	$60\sqrt{2}$ m
Central location of user group	(60 m,10 m)
BS transmit power	30 dBm

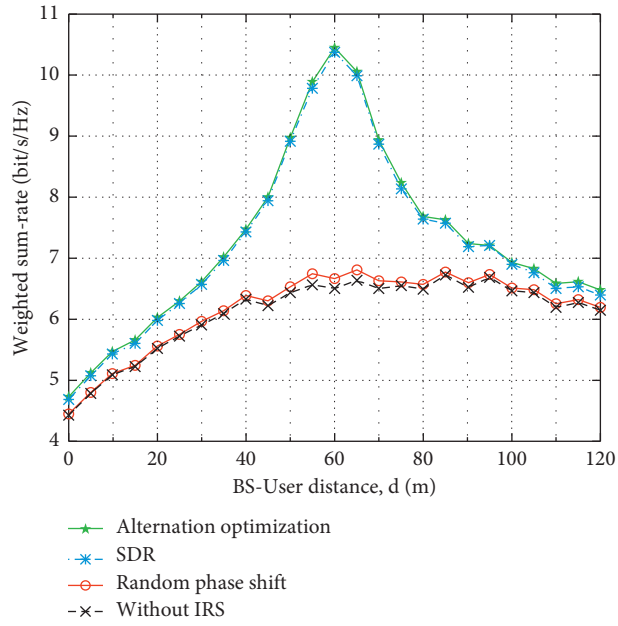

Figure 4: Change curve of achievable rate with distance.

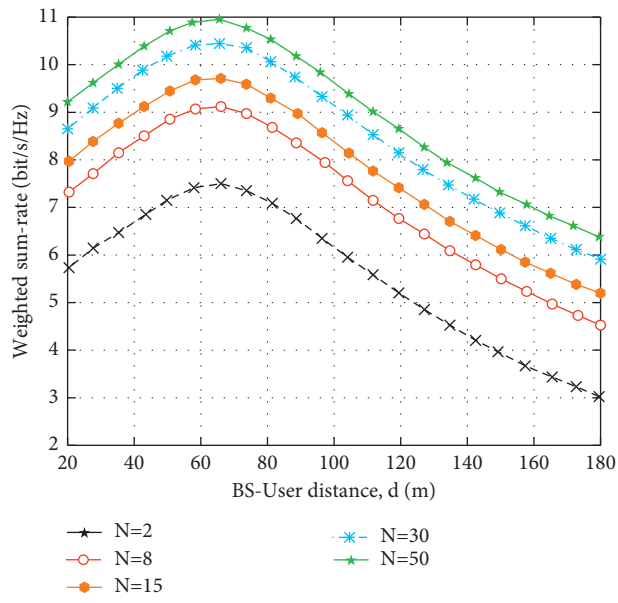

Figure 5: Change curve of achievable rate with distance.

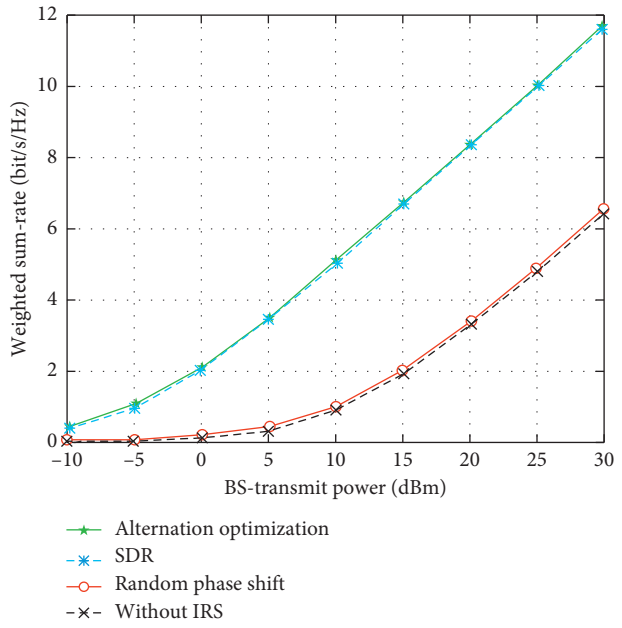

Figure 6: Change curve of the achievable rate with the BS transmit power.

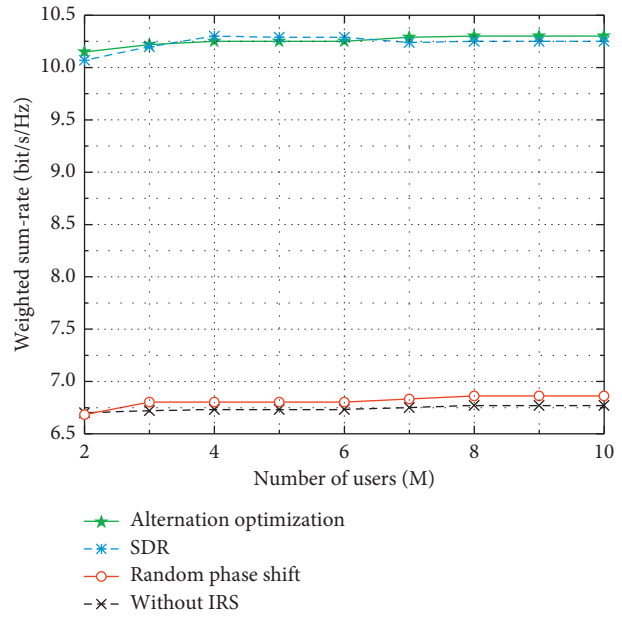

Figure 7: Change curve of the achievable rate with the number of users.

becomes higher as the number of transmitting antennas of BS extends, revealing that increasing the number of antennas of the base station contributes to boosting the signal's achievable rate required by the user.

The link between the signal's achievable rate and the BS's maximum transmit power threshold is depicted in Figure 6. According to the simulation results, the signal's attainable rate will increase monotonically when the BS maximum transmit power threshold increases in all circumstances. Specifically, as the BS transmit power threshold rises, the amount of power allocated to users expands, leading to an increasing attainable rate of the signal required by the user. Furthermore, it can be observed that the signal with the suggested algorithm can attain the maximum rate under the same conditions since the SDR algorithm and the AO algorithm can modulate the reflection phase shift of each reflection unit on the IRS to direct the signal point to a specific user. Therefore, optimizing the reflected phase shift while increasing the BS maximum transmit power threshold might raise the attainable rate of the signal required by the user to a higher extent.

Figure 7 depicts the relationship between the weighted sum rate and the number of users. The results show that as the number of users increases, the weighted sum rate is almost constant, which also means that the average speed of signal transmission to the user decreases.

Figure 8 shows that the weighted sum rate can converge to a stable value when using four transmission schemes for the system. Due to the without IRS and IRS phase-shift randomness, pilot training of IRS is not required before data transmission, so the convergence speed of these two schemes is faster. When using the two schemes of SDR and AO algorithm, in order to achieve more efficient data transmission, it is necessary to conduct pilot training for IRS

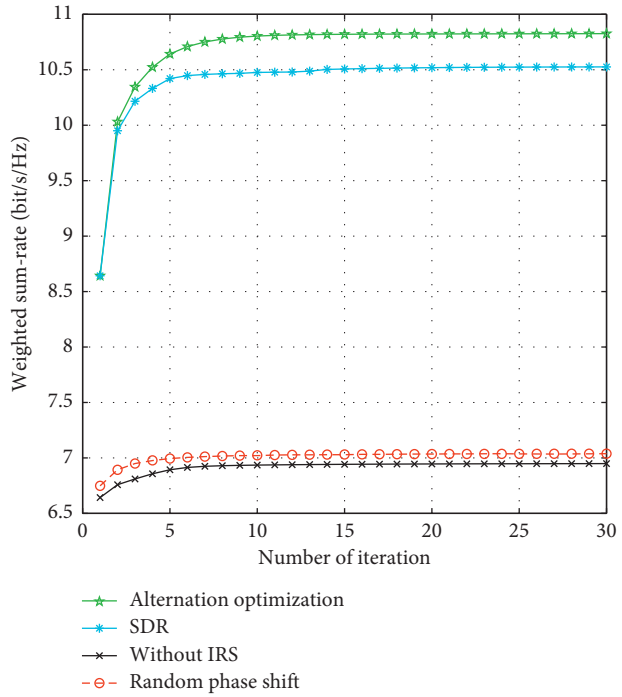

Figure 8: Change curve of the achievable rate with the number of iteration.

before data transmission to ensure that IRS will send signals to users in a more concentrated manner. Therefore, compared with the benchmark scheme, the convergence rate is slower.

Figure 9 describes the link between the number of IRS's reflection units and the signal's achievable rate under the premise of a given maximum transmit power threshold in BS. It can be noticed in the figure that the achievable signal

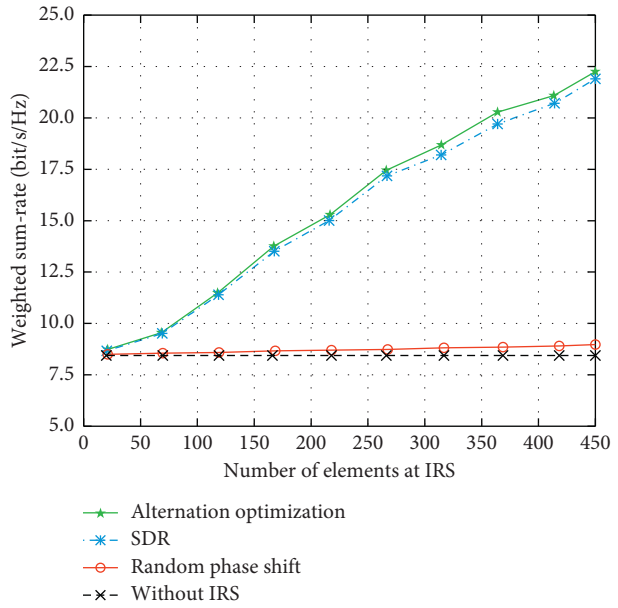

Figure 9: Change curve of the achievable rate with the number of reflecting units.

rate of the IRS-assisted system increases with the growing number of IRS reflection units as a result of an enhanced signal strength required by the user, which is due to the setting of IRS in the system. At the same time, the attainable rate of the system signal using the improved algorithm suggested in this study is much higher than that of the IRS random phase. It shows that as the number of IRS reflection units increases, when the reflection phase shift matrix of the IRS has an optimal value, the signal's rate performance required by the user in the assisted system is optimized, thereby achieving a higher gain. In addition, the algorithm proposed in the paper acquires a significant rate gain when the reflection unit is larger since more IRS reflection units will accordingly reflect the greater power of the signal received from the base station, resulting in more significant power gain. Besides, it can be drawn from the figure that in the NOMA downlink transmission system without IRS assistance, the signal's achievable rate required by the user does not change with the increasing number of IRS reflection units.

5. Conclusion

In response to the IRS-aided NOAM downlink transmission system, this paper adopts two schemes of semidefinite relaxation and alternating optimization, thereby maximizing the achievable rate of the signal required by the user. Given the multivariate coupling of the original problem and the nonconvex constraints, the solving process is quite complex. Therefore, this paper exploits the characteristics of the optimization problem to deduce the relationship between the BS transmit beamforming and the IRS reflection phase shift matrix, further converting the situation into a linear programming problem expecting to reduce the difficulties in the solution process. Furthermore, the SDR algorithm and AO algorithm are used to optimize the transmit beamforming, as well as the reflection phase shift matrix. The simulation results show that compared with the IRS random phase shift system and the system without IRS, the two optimization methods proposed in this paper can significantly enhance the achievable rate of the signal required by the user, indicating that using a large number of reflection units at the IRS while optimizing the phase shift is effective.

Data Availability

The data used to support the findings of this study are included within the article.

Conflicts of Interest

The authors declare that they have no conflicts of interest.

Acknowledgments

This work was partially supported in part by the Science and Technology Department of Gansu Province Project, (Grant Nos. 20JR5RA397, 20JR5RA387, 21JR7RA290, and 20JR5RA387); and in part by InnovationFund for Project of Gansu Provincial Higher Education (2021B-107); and in part by the National Natural Science Foundation of China (62161016, 61661025, and 61901201).

References

[1] S. Singh, D. Mitra, and R. Baghel, "Analysis of NOMA for future cellular communication," in *proceedings of the 2019 3rd International Conference on Trends in Electronics and Informatics (ICOEI), F*, IEEE, Tirunelveli, India, 2019.

[2] Y. Liu, G. Pan, H. Zhang, and M Song, "On the capacity comparison between MIMO-NOMA and MIMO-OMA," *IEEE Access*, vol. 4, pp. 2123–2129, 2016.

[3] L. Dai, B. Wang, Y. Yuan, and S. I. Z Han, "Non-orthogonal multiple access for 5G: solutions, challenges, opportunities, and future research trends," *IEEE Communications Magazine*, vol. 53, no. 9, pp. 74–81, 2015.

[4] L. Dai, B. Wang, Z. Ding, and Z. S. L Wang, "A survey of non-orthogonal multiple access for 5G," *IEEE communications surveys & tutorials*, vol. 20, no. 3, pp. 2294–2323, 2018.

[5] S. Mounchili and S. Hamouda, "Pairing distance resolution and power control for massive connectivity improvement in NOMA systems," *IEEE Transactions on Vehicular Technology*, vol. 69, no. 4, pp. 4093–4103, 2020.

[6] E. G. Larsson, O. Edfors, F. Tufvesson, and T. L Marzetta, "Massive MIMO for next generation wireless systems," *IEEE Communications Magazine*, vol. 52, no. 2, pp. 186–195, 2014.

[7] L. Lu, G. Y. Li, A. L. Swindlehurst, and A. R Ashikhmin, "An overview of massive MIMO: benefits and challenges," *IEEE journal of selected topics in signal processing*, vol. 8, no. 5, pp. 742–758, 2014.

[8] M. Kamel, W. Hamouda, and A. Youssef, "Ultra-dense networks: a survey," *IEEE Communications Surveys & Tutorials*, vol. 18, no. 4, pp. 2522–2545, 2016.

[9] G. Chopra, S. Jain, and R. K. Jha, "Possible security attack modeling in ultradense networks using high-speed handover management," *IEEE Transactions on Vehicular Technology*, vol. 67, no. 3, pp. 2178–2192, 2018.

[10] M. Baghani, S. Parsaeefard, M. Derakhshani, and W Saad, "Dynamic non-orthogonal multiple access and orthogonal multiple access in 5G wireless networks," *IEEE Transactions on Communications*, vol. 67, no. 9, pp. 6360–6373, 2019.

[11] M. Cui, G. Zhang, and R. Zhang, "Secure wireless communication via intelligent reflecting surface," *IEEE Wireless Communications Letters*, vol. 8, no. 5, pp. 1410–1414, 2019.

[12] Q. Wu and R. Zhang, "Towards smart and reconfigurable environment: intelligent reflecting surface aided wireless network," *IEEE Communications Magazine*, vol. 58, no. 1, pp. 106–112, 2020.

[13] Q. Wu, S. Zhang, B. Zheng, C. You, and R. Zhang, "Intelligent reflecting surface aided wireless communications: a tutorial [J]," *IEEE Transactions on Communications*, vol. 69, no. 5, pp. 3313–3351, 2021.

[14] Q. Tao, J. Wang, and C. Zhong, "Performance analysis of intelligent reflecting surface aided communication systems," *IEEE Communications Letters*, vol. 24, no. 11, pp. 2464–2468, 2020.

[15] W. Long, R. Chen, M. Moretti, W. Zhang, and J. Li, "A promising technology for 6G wireless networks: intelligent reflecting surface [J]," *Journal of Communications and Information Networks*, vol. 6, no. 1, pp. 1–16, 2021.

[16] A. S. d Sena, D. Carrillo, and F. Fang, P H. J Nardelli, D B da Costa, U S Dias, Z Ding, C B Papadias, and W Saad, What role do intelligent reflecting surfaces play in multi-antenna non-orthogonal multiple access?" *IEEE Wireless Communications*, vol. 27, no. 5, pp. 24–31, 2020.

[17] F. Fang, Y. Xu, Q.-V. Pham, and Z Ding, "Energy-efficient design of IRS-NOMA networks," *IEEE Transactions on Vehicular Technology*, vol. 69, no. 11, pp. 14088–14092, 2020.

[18] J. Zhu, Y. Huang, J. Wang, and K. Z Navaie, "Power efficient IRS-assisted NOMA," *IEEE Transactions on Communications*, vol. 69, no. 2, pp. 900–913, 2021.

[19] Y. Cheng, K. H. Li, Y. Liu, and K. C. Tec, "Outage performance of downlink IRS-assisted NOMA systems," in *proceedings of the GLOBECOM 2020-2020 IEEE Global Communications Conference, F*, IEEE, Taiwan, China, 2020.

[20] H. Wang, C. Liu, Z. Shi, Y. Fu, and R. Song, "On power minimization for IRS-aided downlink NOMA systems," *IEEE Wireless Communications Letters*, vol. 9, no. 11, pp. 1808–1811, 2020.

[21] Z. Ding and H. Vincent Poor, "A simple design of IRS-NOMA transmission," *IEEE Communications Letters*, vol. 24, no. 5, pp. 1119–1123, 2020.

[22] Z. Ding, R. Schober, and H. V. Poor, "On the impact of phase shifting designs on IRS-NOMA," *IEEE Wireless Communications Letters*, vol. 9, no. 10, pp. 1596–1600, 2020.

[23] X. Mu, Y. Liu, L. Guo, and J. N Lin, "Exploiting intelligent reflecting surfaces in NOMA networks: joint beamforming optimization," *IEEE Transactions on Wireless Communications*, vol. 19, no. 10, pp. 6884–6898, 2020.

[24] Z. Zhang, L. Dai, X. Chen et al., "Active RIS vs. passive RIS: which will prevail in 6G? [J]," arXiv preprint arXiv: 210315154, 2021.

[25] S. Jiao, F. Fang, X. Zhou, and H. Zhang, "Joint beamforming and phase shift Design in downlink UAV networks with IRS-assisted NOMA [J]," *Journal of Communications and Information Networks*, vol. 5, no. 2, pp. 138–149, 2020.

[26] Z. Wang, L. Liu, and S. Cui, "Channel estimation for intelligent reflecting surface assisted multiuser communications," in *proceedings of the 2020 IEEE Wireless Communications and Networking Conference (WCNC), F*, IEEE, Seoul, Korea, 2020.

[27] L. Bariah, S. Muhaidat, P. C. Sofotasios, and S. W. H Gurugopinath, "Non-orthogonal multiple access in the presence of additive generalized Gaussian noise," *IEEE Communications Letters*, vol. 24, no. 10, pp. 2137–2141, 2020.

[28] K. Higuchi and A. Benjebbour, "Non-orthogonal multiple access (NOMA) with successive interference cancellation for future radio access," *IEICE - Transactions on Communications*, vol. E98.B, no. 3, pp. 403–414, 2015.

[29] C. H. Bennett, I. Devetak, A. W. Harrow, and P. W. A Shor, "The quantum reverse Shannon theorem and resource tradeoffs for simulating quantum channels," *IEEE Transactions on Information Theory*, vol. 60, no. 5, pp. 2926–2959, 2014.

[30] O. Mehanna, K. Huang, B. Gopalakrishnan, and A. N. D Konar, "Feasible point pursuit and successive approximation of non-convex QCQPs," *IEEE Signal Processing Letters*, vol. 22, no. 7, pp. 804–808, 2015.

[31] J. Park and S. Boyd, "General heuristics for nonconvex quadratically constrained quadratic programming [J]," arXiv preprint arXiv:170307870, 2017.

[32] D. Adionel Guimaraes, G. H. Faria Floriano, and L. Silvestre Chaves, "A tutorial on the CVX system for modeling and solving convex optimization problems," *IEEE Latin America Transactions*, vol. 13, no. 5, pp. 1228–1257, 2015.

[33] Z. Yang, W. Xu, C. Huang, and J. M Shi, "Beamforming design for multiuser transmission through reconfigurable intelligent surface," *IEEE Transactions on Communications*, vol. 69, no. 1, pp. 589–601, 2021.

[34] O. I. Khalaf and G. M. Abdulsahib, "Frequency estimation by the method of minimum mean squared error and P-value distributed in the wireless sensor network [J]," *Journal of Information Science and Engineering*, vol. 35, no. 5, pp. 1099–1112, 2019.